


H. FURUSAWA
T. SAKKA 
Y. H. OGATA

Characterization of laser-induced plasma plume: Comparison between Al and Al₂O₃ targets

Institute of Advanced Energy, Kyoto University, Uji, Kyoto 611-0011, Japan

Received: 29 September 2003/Accepted: 4 March 2004
Published online: 26 July 2004 • © Springer-Verlag 2004

ABSTRACT Characterization of the plasma plume produced by laser ablation from Al and Al₂O₃ targets was carried out on the basis of the line profile analysis of Al(I) (²P°–²S) emission. The spatial distribution and density parameters of electrons and Al atoms in the plume were obtained by comparing observed spectral line profiles with a theoretical calculation. The results showed different behavior for the Al and Al₂O₃ targets. The Al atoms from the Al₂O₃ target were populated in a smaller region than those from the Al target.

PACS 52.38.MF; 52.70.Kz; 52.25.Os

1 Introduction

Laser ablation has attracted much interest in material processing, such as thin film fabrication and fine particle formation [1–4]. Furthermore, highly active species obtained by the laser ablation process can be used for various chemical reactions. Many studies on the characterization of ablated species have been performed [3–8]. The spatial distribution of ablated species is an important parameter for the investigation of the above applications. In addition, the density of electrons and chemically reactive species affects the kinetics of the chemical reactions in the plume.

So far, we have performed the studies on laser ablation under atmospheric pressure conditions, which has the advantage of confining highly energetic ablated species by ambient gases, leading to an increase in the collision frequency between ablated and ambient species [9–11]. We have been studying the ablated species by emission spectroscopy. The density of the plasma plume produced under a high pressure ambient gas is very high, and strong self-absorption is evident in emission spectra. This strong self-absorption must be understood minutely for analysis based on spectroscopy. The feature of a spectral line profile is very sensitive to the spatial population distribution of the atoms involved in the emission and absorption. We have developed a model based on the analysis of radiative transfer, and have shown that the density of electrons and the ablated species, and their spatial distribution can be obtained by fitting to experimental line profiles [11].

In the present work, ablated species from Al₂O₃ is compared to those from Al, and the difference is discussed. Two emission lines of Al (I) originating from the fine structure doublet, ²P°_{1/2}–²S_{1/2} (394.401 nm) and ²P°_{3/2}–²S_{1/2} (396.152 nm), were measured. The time-resolved analysis was carried out by reproducing the spectral line profile observed at each delay time. The results enabled us to conclude that the behavior of Al atoms in the plume depends on a target, Al or Al₂O₃.

2 Experimental

The target chamber was equipped with a rotary pump for evacuation, a line for gas introduction, and a quartz window for laser irradiation. Nitrogen gas was used as an ambient gas. The chamber was filled with N₂ gas up to a pressure of 760 Torr after evacuation. The pressure was measured by a capacitance type pressure gauge. The laser ablation was performed using a 30 mJ pulse of a Nd:YAG laser with a pulse duration of 20 ns. The laser beam was focused by a lens with a focal length $f = 10$ cm, and irradiated onto an aluminum target (99.9999%, Nilaco Co.) or a sintered α -alumina target (99.99%, Nilaco Co.) placed in the chamber.

For the measurement of the spectral line profile, the emission from the plume was introduced to the entrance slit of the spectrograph. A one meter focal-length double dispersion spectrograph (Ritsu Oyo Kogaku, MC100N) equipped with two 1800 grooves/mm diffraction gratings was used. The slit with 20 μ m in width was arranged perpendicular to the target surface. An intensified charge coupled device (ICCD) (Princeton Instrument, ICCD-1024MTDGE/1) was used as a detector. The spectral resolution of this system was 0.04 nm. Duration of the time gate to operate the ICCD detector was 20 ns and the time delay from the laser pulse was varied from 100 to 5000 ns.

Because the information about the plume size is required for the model calculation, the lateral imaging experiment on the plume was carried out by using the ICCD with a camera lens installed. The size of the plume was obtained by fitting the intensity profile of the image to Gaussian function.

3 Analysis

The model is based on a one-dimensional radiative transfer calculation. The details of the calculation are given

✉ Fax: +81-774/38-3499, E-mail: t-sakka@iae.kyoto-u.ac.jp

in [11]. In the calculation, we assumed that the density distribution of plasma electrons and the population distributions of Al atoms are independent from each other. The spectral profiles were reproduced by adjusting the parameters appearing in the distribution functions. By following our previous work [11], we assumed a Gaussian distribution for the plasma free electrons and the populations along the axis parallel to the target, i.e.,

$$n_e(x) = N_{e0} \exp\left(-\frac{x^2}{\sigma_e^2}\right)$$

$$n_1(x) = N_{10} \exp\left(-\frac{x^2}{\sigma_1^2}\right)$$

$$n_2(x) = N_{20} \exp\left(-\frac{x^2}{\sigma_2^2}\right)$$

where $n_e(x)$, $n_1(x)$, and $n_2(x)$ are the electron density and the population densities at the lower and upper levels, respectively. The width parameters σ_e , σ_1 , and σ_2 are for the electrons and the atoms at the lower and upper levels, respectively, and N_{e0} , N_{10} , and N_{20} are their maximum densities at $x = 0$. By applying the same assumptions as in our previous paper [11], N_{e0} , N_{10} , and σ_1 were selected to be adjustable parameters.

An intuitive understanding of the self-reversed profile [11, 12] can be made by considering the absorption of the emitted light near the center of the plume by a relatively-cold peripheral region. If the peripheral region is not cold enough, or the spatial population distribution is extinguished without experiencing the cold periphery, the self-reversed profile is not expected.

4 Results

In Fig. 1, examples of the emission line profiles are shown. Regardless of the target, the profiles with clear emission lines were not observed until 100 ns after the irradiation because of a strong continuous spectrum. The intensity ratio of the two emission lines assigned to the fine-structure doublet of Al was far from unity until 400 ns. However, the intensity ratio later became almost unity in the case of the Al target, but not in the case of the Al_2O_3 target. The self-reversed structure was observed in the profiles when the ratio was nearly unity in the case of the Al target. On the other hand, the self-reversed structure was hardly observed in the case of the Al_2O_3 target throughout the observation time.

The model calculation successfully reproduced the spectral line profiles. The parameters obtained by the fitting process are shown in Fig. 2. The electron density parameter N_{e0} decreased with time, and showed the same behavior for the Al and Al_2O_3 target (Fig. 2a). The dependence of the target material appeared in the parameters for Al population, namely, N_{10} and σ_1 . The population density parameter N_{10} obtained in the case of Al ablation was almost constant, ca. $2 \times 10^{22} \text{ m}^{-3}$, throughout the observation time range. On the other hand, for the Al_2O_3 ablation, it was the same value as that for the Al ablation until 400 ns, but gave higher values of ca. $6 \times 10^{22} \text{ m}^{-3}$ in the later time range (Fig. 2b). The spatial distribution parameter σ_1 was larger for the Al ablation than that of the Al_2O_3

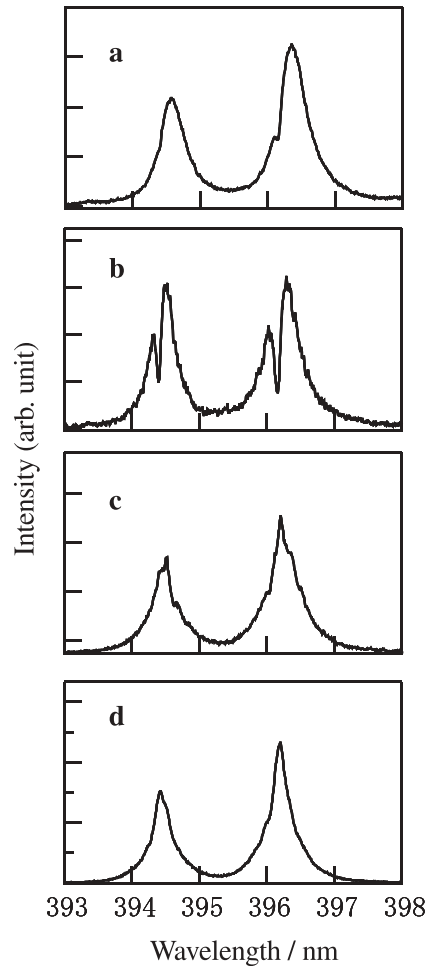


FIGURE 1 Emission line profiles of ${}^2P^{\circ}_{1/2}-{}^2S_{1/2}$ (394.401 nm) and ${}^2P^{\circ}_{3/2}-{}^2S_{1/2}$ (396.152 nm) from **a,b**, Al, and **c,d**, Al_2O_3 , ablation in N_2 atmosphere observed at **a,c**, 200 ns, and **b,d**, 600 ns

ablation (Fig. 2c). In both cases, it was almost independent of time within the scattering of the data points.

5 Discussion

The spectral line profiles given in Fig. 1 clearly suggest the target effects on the behavior of the ablated species in the plume. The ratio of the peak intensity of the 394 nm line to that of the 396 nm line can be an indicator of the population density. A high population density causes a high optical thickness of the plume, resulting in the ratio approaching unity, regardless of the original ratio of 0.5. For the Al ablation, the population density was sufficient to give the ratio of unity after 400 ns, while it was rather small for self-absorption to apparently occur in the Al_2O_3 ablation plume. In addition, the self-reversed structure suggests self-absorption at a cold periphery, or strong absorption in the peripheral region of the plume. For the plume produced by Al ablation, strong self-absorption seemed to occur in the peripheral region, while it was not effective in the plume produced by Al_2O_3 ablation.

In addition to the qualitative discussion of the spectral line profiles, quantitative information about the ablated species was obtained by the model calculation. As for the electron density parameter N_{e0} , the difference between the targets was

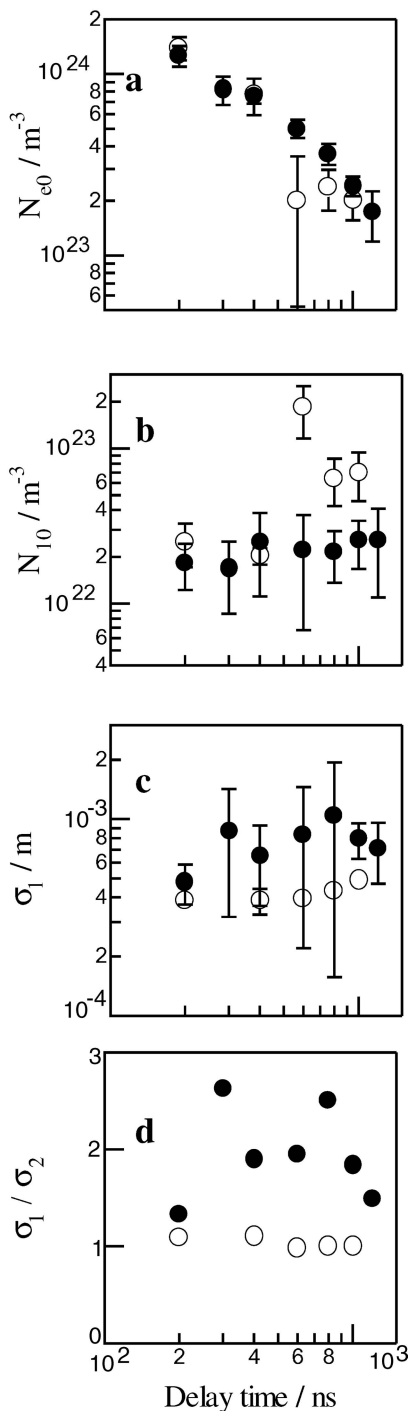


FIGURE 2 The best-fit parameters obtained by fitting the spectral line profiles observed for the (●) Al and the (○) Al₂O₃ ablation in N₂ atmosphere to the theoretical ones. The parameters N_{e0} (a), N_{10} (b), and σ_1 (c) are shown. The ratio of the spatial distribution widths of the populations involved in the transition, σ_1/σ_2 , is given in d

not seen. However, population density and its widths of spatial distribution differed for the two targets. For the Al₂O₃ ablation, N_{10} was higher, and σ_1 was smaller than that for the Al ablation. This is not inconsistent with the results discussed above that the plume from the Al target shows a higher optical density than for Al₂O₃ ablation, since the optical density is a function not only of the density but also of the geometri-

cal thickness. Figure 2c indicates that the Al atoms from the Al₂O₃ target are present in a region smaller than the Al target. This indicates that in the present specific case the contribution of the spatial distribution is very important in determining the optical thickness.

The ratio σ_1/σ_2 is shown in Fig. 2d. It represents the ratio of the spatial distribution widths of the populations at the upper and the lower levels. For the Al₂O₃ ablation, the ratio was almost constantly unity throughout the observation time range. For the Al ablation, it ranged from 1.3 to 2.6, while a clear time dependence was not observed. In the plume produced by the Al₂O₃ ablation, the populations at the upper and lower levels existed in almost the same region, resulting in weak self-absorption in the plume periphery. This is consistent with the spectral line profiles which did not have the self-reversed structure. On the other hand, the population at the lower level spread more widely than that at the upper level in the plume of the Al ablation. This resulted in the strong self-absorption in the peripheral region, and hence the self-reversed structure in the spectral line profiles.

Generally, the characteristics of the laser ablation plume are sensitive to the irradiation condition, especially to the pulse energy given to the target surface. Although our irradiation condition is the same for both targets, it does not guarantee the same amount of energy deposited on the surface, due to the difference in the laser surface interaction. However, the difference in the absorbed energy cannot fully explain the present results, since a large amount of energy is expected to give a high electron density, a high atomic density, and also a large distribution of the ablated species. The present results, especially the difference in the width of the spatial distribution, are consistently explained by the melting point of the target. In the Al ablation, thermal evaporation strongly contributed to the ablation process due to the lower melting point of Al. Many more Al atoms at the ground state were evaporated in a longer time duration than in the Al₂O₃ ablation, and distributed widely. Since the melting point of Al₂O₃ is high, the thermal evaporation of Al₂O₃ would not be so enhanced as for Al.

6 Conclusion

The difference in the ablation behavior of the Al and Al₂O₃ target was clarified by the analysis of the Al(I) ²P^o-²S emission line profiles on the basis of the radiative transfer calculation. The results clearly showed that the distribution of the population was larger in the Al ablation than in the Al₂O₃ ablation. This is explained by the lower melting point of Al metal, which results in an intense thermal evaporation.

ACKNOWLEDGEMENTS We would like to acknowledge Kouchi Hotta and Yoshiyuki Nishinosono for technical support. This work is financially supported by the Grant-in-Aid for Scientific Research from the Japanese Society for the Promotion of Science.

REFERENCES

- 1 J.C. Miller: *Laser Ablation: Principles and Applications*, J.C. Miller (ed.) (Springer Verlag, Berlin 1994) p. 1
- 2 R.F. Haglund, Jr., N. Itoh: *Laser Ablation: Principles and Applications*, J.C. Miller (ed.) (Springer Verlag, Berlin 1994) p. 11

- 3 T. Sasaki, S. Terauchi, N. Koshizaki, H. Umehara: Appl. Surf. Sci. **127–129**, 398 (1998)
- 4 D.B. Geohegan, A.A. Puretzky, D.J. Rader: Appl. Phys. Lett. **74**, 3788 (1999)
- 5 T. Makimura, K. Murakami: Appl. Surf. Sci. **96–98**, 242 (1996)
- 6 Y. Franghiadakis, C. Fotakis, P. Tznetakis: Appl. Phys. A. **68**, 391 (1999)
- 7 K. Sasaki, T. Wakasaki, S. Matsui, K. Kadota: J. Appl. Phys. **91**, 4033 (2002)
- 8 B. Toftmann, J. Schou, T.N. Hansen, J.G. Lunney: Phys. Rev. Lett. **84**, 3998 (2000)
- 9 T. Sakka, S. Iwanaga, Y.H. Ogata, A. Matsunawa, T. Takemoto: J. Chem. Phys. **112**, 8645 (2000)
- 10 K. Saito, K. Takatani, T. Sakka, Y.H. Ogata: Appl. Surf. Sci. **197–198**, 56 (2002)
- 11 T. Sakka, T. Nakajima, Y.H. Ogata: J. Appl. Phys. **92**, 2296 (2002)
- 12 J. Hermann, C. Boulmer-Laborgne, D. Hong: J. Appl. Phys. **83**, 691 (1998)